J. Membrane Biol. 173, 139–148 (2000)

The Journal of
Membrane
Biology

Effects of Cationic Substitutions on Delayed Rectifier Current in Type I Vestibular Hair Cells

K.J. Rennie[1], **M.J. Correia**[1,2]

Departments of Otolaryngology[1] and Physiology and Biophysics[2], The University of Texas Medical Branch, Galveston, Texas 77555, USA

Received: 23 June 1999/Revised: 27 September 1999

Abstract. The resting potassium current (I_{KI}) in gerbil dissociated type I vestibular hair cells has been characterized under various ionic conditions in whole cell voltage-clamp. When all K^+ in the patch electrode solution was replaced with Na^+, $(Na^+)_{in}$ or Cs^+, $(Cs^+)_{in}$, large inward currents were evoked in response to voltage steps between −90 and −50 mV. Activation of these currents could be described by a Hodgkin-Huxley-type kinetic scheme, the order of best fit increasing with depolarization. Above ~ −40 mV currents became outward and inactivated with a monoexponential time course. Membrane resistance was inversely correlated with external K^+ concentration. With $(Na^+)_{in}$, currents were eliminated when K^+ was removed from the external solution or following extracellular perfusion of 4-aminopyridine, indicating that currents flowed through I_{KI} channels. Also, reduction of K^+ entry through manipulation of membrane potential reduced the magnitude of the outward current. Under symmetrical Cs^+, 0 K^+ conditions I_{KI} is highly permeable to Cs^+. However, inward currents were reduced when small amounts of external K^+ were added. Higher concentrations of K^+ resulted in larger currents indicating an anomalous mole fraction effect in mixtures of external Cs^+ and K^+.

Key words: Semicircular canal — Utricle — Gerbil — Potassium channel — Anomalous mole fraction

Introduction

In the vestibular end organs of higher vertebrates there are two types of sensory hair cell, namely type I and type II. Properties that distinguish the two hair cell types include their innervation and cellular morphology (Wersäll, 1956; Ricci et al., 1997*a,b*; Rüsch, Lysakowski & Eatock, 1998). Type II hair cells, juxtaposed to supporting cells, are contacted by afferent and efferent bouton endings. Type I hair cells in contrast are surrounded by a cup-shape afferent nerve calyx and receive no direct efferent innervation, although efferent fibers make synaptic contact with the outer faces of calyces. In addition there are significant differences between the membrane properties of type I and type II hair cells. These observations suggest that the two cell types play distinct roles in the processing of vestibular signals.

All mature type I cells have a low-voltage activated delayed rectifier K^+ conductance I_{KI} or I_{KL}, (Rennie & Correia, 1994; Rüsch & Eatock, 1996*a*; Ricci, Rennie & Correia, 1996). It activates at potentials between −100 and −80 mV and is typically about 50% activated at the zero-current potential, which in gerbil type I hair cells is close to −70 mV (Rennie & Correia, 1994). The presence of this conductance confers upon type I hair cells a low input resistance. Additional K^+ conductances have also been reported in these cells. At potentials above approximately −55 mV, a second delayed rectifier current is present in type I hair cells of the neonatal mouse utricle (Rüsch & Eatock, 1996*a*; Rüsch et al., 1998). In gerbil semicircular canal hair cells, a calcium-dependent K^+ current is present above ~ −40 mV (Rennie & Correia, 1994). Since both conductances are active at potentials far depolarized from rest, their physiological significance remains unclear. Two classes of inward rectifier channel have also been identified in the mouse utricle (Rüsch et al., 1998). However, I_{KI} is the dominant resting conductance and it is predicted to allow type I cells to respond rapidly and with a low sensitivity to transduction signals. Variations in the magnitude of I_{KI} have led to suggestions that this current may be subject to physiological modulation and recently, I_{KI} in rat vestibular hair cells has been shown to be under second messenger control via a cGMP-mediated pathway (Behrend et al., 1997).

Correspondence to: K.J. Rennie

K^+ ions are involved in a number of roles in hair cell function; they are the main charge carriers of the transduction current and many of the basolateral conductances found in different hair cells are K^+ selective (for review *see* Correia, Ricci & Rennie, 1996). In the case of type I hair cells, a combination of the restricted intercellular space between the type I hair cell and its calyx and the large size of I_{KI} may result in K^+ levels that change by several millimolar during natural stimulation (Goldberg, 1996*a*,*b*).

The purpose of this study was to investigate the permeation properties of the type I hair cell I_{KI} conductance under various ionic conditions. An examination of the permeation properties of this channel should provide insight not only into its functional capabilities, but also into its molecular structure. We show that even when K^+ ions are absent from the patch electrode solution, large bidirectional currents are seen under whole cell patch-clamp conditions in the presence of external K^+. In external solutions of different mixtures of K^+ and Cs^+ a mole fraction effect is seen indicating that the channel is a multi-ion pore.

Materials and Methods

Cell Isolation

Type I hair cells were extracted from the semicircular canals and utricles of Mongolian gerbils using modifications of previously described techniques (Rennie & Correia, 1994; Rennie, Ricci & Correia, 1996). Animals were deeply anesthetized (Nembutal 40 mg/kg ip, ketamine 40 mg/kg im) and the membranous labyrinth was exposed by breaking through the bullae and bony labyrinth. The semicircular canals and utricle were carefully removed using fine forceps and iris scissors and were immersed in a chilled high Mg^{2+}/low Ca^{2+} solution containing (in mM): NaCl (135), KCl (5), $MgCl_2$ (10), $CaCl_2$ (0.02), NaH_2HPO_4 (2), Na_2HPO_4 (8) and D-glucose (3). Animals were decapitated immediately following end organ removal. The crista ampullaris was trimmed from surrounding tissue and the otolithic membrane was removed from the utricle. Tissue was then left for 30–35 minutes in the high Mg^{2+}/low Ca^{2+} solution at 37°C. No enzymes were used in the dissociation process. Epithelia were transferred to Leibovitz's L-15 medium (Life Technologies) containing bovine albumin (1 mg/ml), for a minimum of 50 min at room temperature. Individual end organs were then transferred to a small volume of extracellular solution, placed in the recording chamber and hair cells were mechanically dissociated by drawing a probe across the surface of the epithelium. Cells were then left for 10–20 min to settle to the bottom of the recording chamber. Isolated type I hair cells were visually identified by previously established morphometric criteria, i.e., a neck to cuticular plate ratio <0.70 and a neck to body ratio <0.58 (Ricci et al., 1997*a*).

Recording Conditions

Electrodes were pulled from Corning 8161 glass (World Precision Instruments and Warner Instrument) on a Sutter Instruments microelectrode Puller (P-87), fire polished on a microforge (Narashige MF 83) and coated with silicone elastomer (Sylgard, Dow Corning) just prior to use. Electrode solutions contained the following: K^+ solution $(K^+)_{in}$ (total K^+ 152 mM, pH 7.4 with KOH): (in mM) KF (110), KCl (15), NaCl (1), HEPES (10), D-glucose (3), $MgCl_2$ (1.8) and EGTA (10). Na^+ solution $(Na^+)_{in}$ (total Na^+ 137 mM, pH 7.4 with NaOH): NaF (110), HEPES (10), D-glucose (3), $MgCl_2$ (1.8) and EGTA (10). Cs^+ solution $(Cs^+)_{in}$ (total Cs^+ 150 mM, pH 7.4 with NaOH): CsF (150), HEPES (10), D-glucose (3), $MgCl_2$ (1.8) and EGTA (11). The osmolality of intracellular solutions was brought to 300–315 mmol/kg H_2O with sucrose. Normal extracellular solution was (in mM): NaCl (155), KCl (5), $MgCl_2$ (1.8), $CaCl_2$ (1.1), HEPES (10) and D-glucose (3), pH to 7.4 with NaOH. In experiments where the external K^+ concentration $[K^+]_{out}$ was increased, equimolar amounts of Na^+ or Cs^+ were replaced with K^+. Chemicals were purchased from Sigma, except for 4-aminopyridine which was from Fluka. Solution exchange was via whole bath perfusion or gravity-fed local perfusion from an array of flow pipes placed ~100 μm from the cell under study.

Experiments were performed at room temperature (~22°C). The patch-clamp setup included an Axopatch 1C patch amplifier connected to a PC through an AD converter (CED 1401, Cambridge Electronic Design). Data were acquired and analyzed using CED Patch and Voltage Clamp software (v 6). Signals were filtered online at 5 kHz. Electrode resistance was typically 0.5–2.0 MΩ. The series resistance was 4.1 ± 3.1 MΩ (n = 125, mean ± SD) and was electronically compensated up to 80% during recordings. Remaining voltage errors due to uncompensated series resistance were estimated from peak current values and corrected for offline. For the largest currents recorded, the true voltage could potentially vary by as much as 5 mV during a voltage step. Voltages were also corrected for liquid junction potentials. Mean cell capacitance was 3.0 ± 1.2 pF (n = 125). Leakage subtraction was not performed unless stated.

Data Analysis

Cellular membrane resistance was estimated in voltage clamp using the following protocol. The cell was held at or close to −70 mV, since I_{KI} is approximately 50% activated at this potential (Rennie & Correia, 1994). Brief pulses (40 msec duration) in increments of 2.5 mV were applied to step the membrane potential between −80 and −50 mV. The contribution of other conductances at these potentials is minimal (Rennie & Correia, 1994; Rüsch & Eatock, 1996*a*). The current amplitude was measured at <2 msec into each pulse and the slope of the *V-I* relation was fitted by linear regression (Sigmaplot, least squares method). In Fig. 6*D* slope conductance was estimated from the current elicited in response to a voltage ramp where the cell was held at or close to −70 mV and the voltage was ramped at 1 mV/msec to potentials between −90 and −20 mV.

The activation of inward currents was fitted with the following equation:

$$X = A + B(1 - e^{-t/\tau})^n \quad (1)$$

where A is offset, B is magnitude, t is time, τ is the time constant and n is the order.

Results

K^+ Currents in Type I Hair Cells

Figure 1*A* shows the whole cell currents recorded from an isolated type I hair cell when K^+ was the main cation in the patch electrode solution and 10 mM K^+ was present

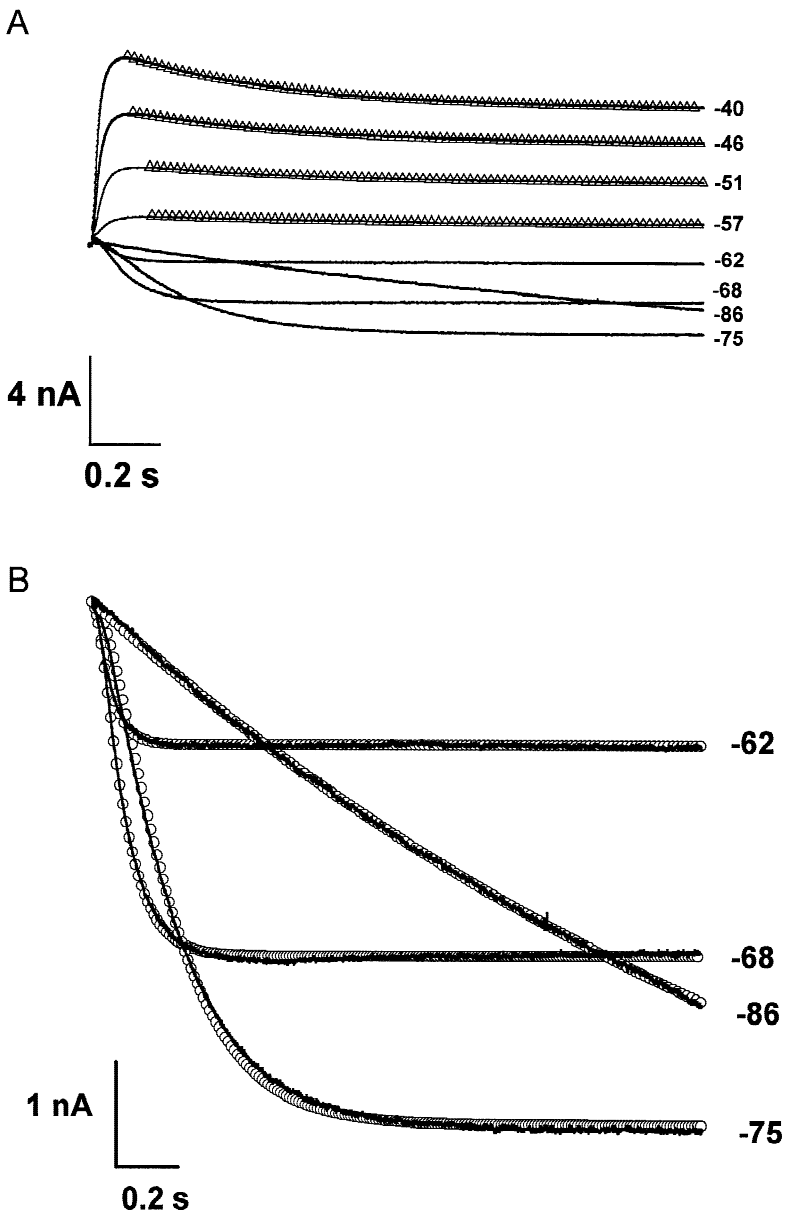

Fig. 1. A large potassium conductance is active at rest in type I hair cells. Whole cell currents with $K^+_{(in)}$ as the electrode solution and 10 mM K^+ in the external solution. (*A*) Type I hair cell was held at −103 mV and stepped to the potentials in mV indicated to the right of current records. Inactivation of the outward currents followed a monoexponential time course. Fits to the raw data are indicated by the open triangles. Inactivation time constants with increasing depolarization were 0.6, 0.52, 0.48 and 0.46 sec. (*B*) Activation of the inward currents was fit with Eq. 1. Best fits are shown by the open circles, every 10th point shown. The step to −86 mV was best fit with an order of 1 and other steps were best fit with $n = 2$.

externally. The cell was held at −103 mV and stepped through a range of depolarized potentials. At −86 mV a slowly developing inward current is seen. Progressively larger depolarizations elicit large inward and then outward currents. The inactivation of outward currents could be fit with a single exponential (open triangles). The currents between −50 and −100 mV have previously been shown to be carried through a low-voltage activated delayed rectifier and give rise to the low input resistance typical of type I hair cells (Rennie & Correia, 1994; Rüsch & Eatock, 1996*a*). The activation of the outward currents has been described previously and in pigeon type I hair cells was fit by a Hodgkin-Huxley type kinetic scheme with an order of 1 (Ricci et al., 1996). The activation of inward currents was fitted with Eq. 1 varying the order between 1 and 4 (open circles, Fig. 1*B*). At the most hyperpolarized potentials an order of 1 produced the best fit, but as the depolarizations increased so did the order of the best fit (Fig. 1*B*).

Intracellular Na^+ Does Not Block K^+ Currents in Type I Hair Cells

To further investigate inward currents carried through I_{KI}, K^+ in the electrode solution was replaced with Na^+. With 5 mM K^+ present externally, large currents were still observed (Fig. 2*A* and *B*). A slowly increasing in-

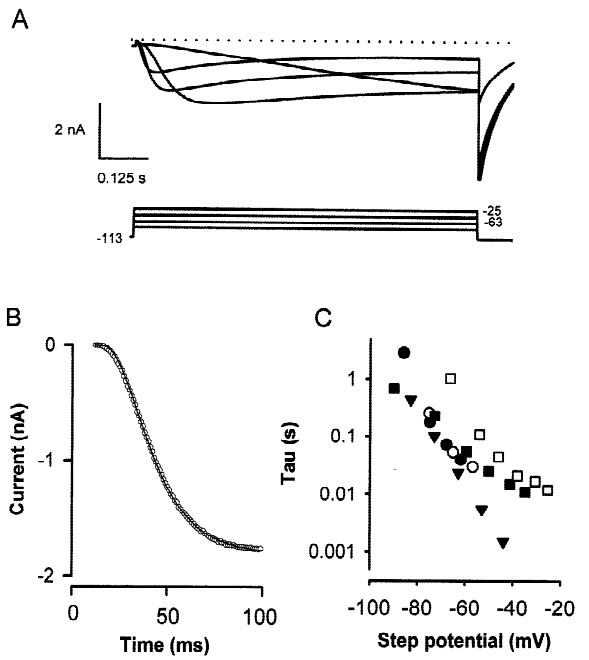

Fig. 2. Inward currents in a type I cell loaded with Na^+ ions. Electrode solution included 137 mM Na^+ and $[K^+]_{out}$ was 5 mM. (*A*) At potentials above approximately −90 mV, a slowly developing inward current was apparent. Activation and inactivation of the current became faster with depolarization. In this cell the membrane potential was held at −113 mV and stepped to −83, −63, −44 and −25 mV. Zero current level in this and subsequent figures is represented by the interrupted line. (*B*) The activation of the inward current in *A* was fit with Eq. 1 and shown for the step to −44 mV (raw data represented by symbols and the fit by the solid line). In this case $n = 4$ produced the best fit ($\tau = 16$ msec). (*C*) Activation time constants for inward currents fitted with Eq. 1 are shown for different cells under a variety of conditions; open circles $(K^+)_{in}$ and 20 mM $[K^+]_{out}$, filled circles $(K^+)_{in}$ and 10 mM $[K^+]_{out}$, filled triangles, (from the cell shown in *A*), $(Na^+)_{in}$ and 5 mM $[K^+]_{out}$, open squares $(Cs^+)_{in}$ and 20 mM $[K^+]_{out}$ and filled squares $(Cs^+)_{in}$ and 5 mM $[K^+]_{out}$. The order of the best fit in all examples shown, with one exception, was 1 at the most hyperpolarized potential shown and increased with depolarizing steps to a maximum value of 4. For the cell represented by the filled triangles, the order of best fit was 2 at −83 mV.

ward current was first seen at potentials above ~ −90 mV. Activation of the inward current became faster and the current began to inactivate with larger depolarizations (Fig. 2*A*). Peak inward current was typically seen at potentials between −60 and −80 mV and the peak amplitude was 2.6 ± 1.6 nA in 5 mM K^+ (mean ± SD, $n = 24$). Reversal of the current typically occurred at potentials between −50 mV and −20 mV. The activation of the inward current was fit with Eq. 1 as shown in the example of Fig. 2*B*. As seen in K^+-filled cells, the order of best fit increased with increasing depolarization. Time constants for activation of the inward currents were similar under a variety of different ionic conditions and are shown in Fig. 2*C*, where the electrode solution was $(K^+)_{in}$ (circles), $(Na^+)_{in}$ (triangles) or $(Cs^+)_{in}$ (squares) and the $[K^+]_{out}$ was 5 or 10 mM (filled symbols) or 20 mM (open symbols).

Outward currents with $(Na^+)_{in}$ activated rapidly and inactivated more slowly (Fig. 3*A*). Inactivation followed a monoexponential time course whose time constant decreased with depolarization (example fits to current records are indicated by the open symbols in Fig. 3*A*). Figure 3*B* shows the mean inactivation time constants of currents with $(Na^+)_{in}$ (gray bars) compared to those with $(K^+)_{in}$ (unfilled bars). Inactivation was faster with $(Na^+)_{in}$ (statistically significant differences are indicated by the asterisks). The maximum amount of inactivation with $(K^+)_{in}$ was about 35% (*not shown*), whereas with $(Na^+)_{in}$ some currents showed complete inactivation (*see* Figs. 3*A* and 6*A*).

Activation kinetics for the inward currents were similar between $(Na^+)_{in}$ and $(K^+)_{in}$ conditions and the role played by external K^+ in the generation of these currents was investigated. Figure 4*A* shows that removal of external K^+ resulted in a marked reduction of both inward (Fig. 4*A*2) and outward (Fig. 4*A*1) currents in cells patch clamped with $(Na^+)_{in}$. Similar results were seen when the main pipette cation was Cs^+ or *N*-methyl-D-glucamine (*not shown*). The membrane currents in response to voltage ramps under the different K^+ concentrations are shown for the same cell in Fig. 4*B*. These results suggested that both inward and outward current components were carried by, or depended upon, the presence of external K^+ ions and were not due to Na^+ ions permeating through the channel as has been described in certain other K^+ channels (Korn & Ikeda, 1995; Kiss et al., 1998). The relationship between the external K^+ concentration and membrane resistance of type I hair cells patch-clamped with $(Na^+)_{in}$ was further investigated and is shown in Fig. 4*C* (filled symbols). Membrane resistance was closely correlated with external K^+ concentration, with high concentrations of external K^+ resulting in minimal values for membrane resistance. Similar results were seen in cells patched with $(Cs^+)_{in}$, when Na^+ was the major extracellular cation and the external K^+ was varied (open symbols, Fig. 4*C*). However, in symmetrical Cs^+, when $(Cs^+)_{in}$ was the pipette solution and external K^+ and Na^+ were replaced with Cs^+, the mean membrane resistance at −70 mV was 19.2 ± 3.8 MΩ ($n = 8$, *data not shown*). This confirms previous observations that I_{KI} is significantly permeable to Cs^+ (Rennie & Correia, 1994; Rüsch & Eatock, 1996*a*). However, as shown below, Cs^+ and K^+ permeability through I_{KI} channels are not independent.

K^+ Loading and Depletion in Conditions of $(Na^+)_{in}[K^+]_{out}$

Typical protocols involved holding the cell at a hyperpolarized potential and stepping to increasingly less

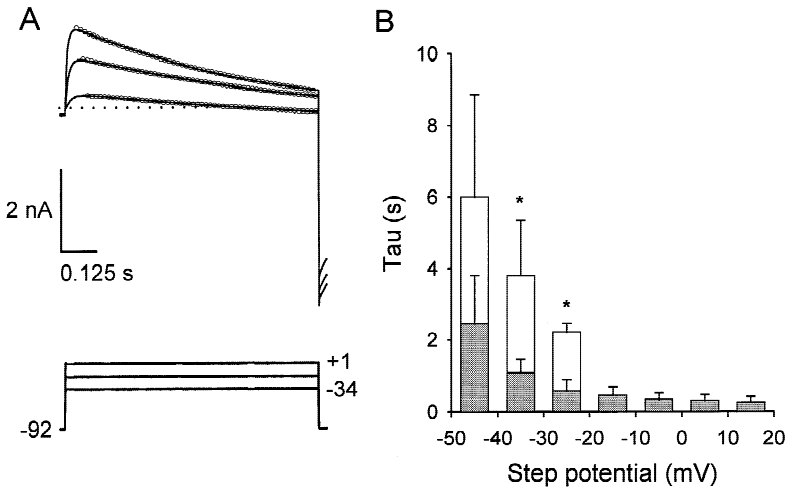

Fig. 3. Inactivation of outward currents in type I cell loaded with Na^+ ions. (*A*) The outward currents rapidly reached a peak value then decayed over the duration of the pulse. Raw data (solid lines) are shown superimposed on monoexponential fits to the outward currents (open symbols, every 15th point shown), with increasing depolarizations tau = 1.22, 1.02 and 0.74 sec. Cell was held at −92 mV and stepped to −34, −16 and +1 mV. (*B*) A histogram showing mean inactivation time constants (tau) of the outward current for $(Na^+)_{in}$ (grey bars) and $(K^+)_{in}$ (unfilled bars) in the presence of 2 mM external K^+. The mean ± 1 SD for 3–5 cells is shown and statistically significant differences are indicated by * (unpaired *t*-test, $P < 0.05$). Bin width is 10 mV.

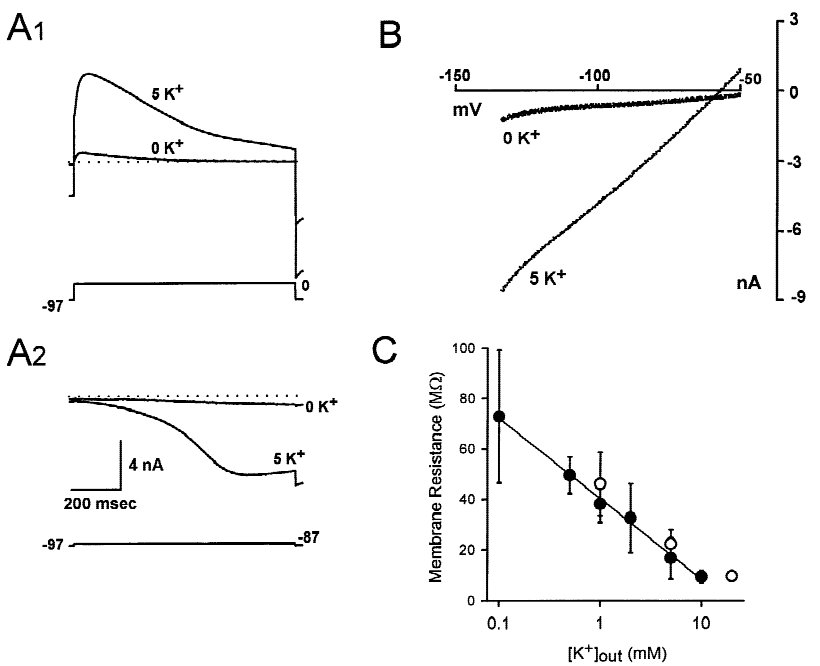

Fig. 4. Effect of changing external K^+ on whole cell currents with no K^+ present in the patch electrode solution. (*A*) In normal extracellular solution ($[K^+]_{out}$ = 5 mM) and $(Na)_{in}$, a depolarizing step evokes a large outward current which rapidly reaches a peak value and then decays (*A*1, current at holding potential indicated by dotted line). Following removal of external K^+, the same step evokes a reduced current whose peak value is less than 10% of the control peak value. The inward current in normal extracellular solution is virtually abolished in 0 K^+ (*A*2). (*B*) Ramp protocols from the same cell shown in *A* in the presence and absence of K^+. Each trace represents the average of 8 stimulus presentations. (*C*) Membrane resistance as a function of external K^+ with $(Na^+)_{in}$ or $(Cs^+)_{in}$ as the electrode solution. Each filled circle represents the mean ± SD for between 4 and 11 cells with $(Na)_{in}$, (regression indicated, r^2 = 0.996) each unfilled circle represents the mean ± SD for 4–5 cells with $(Cs)_{in}$. Membrane resistance was measured in voltage clamp as described in Materials and Methods.

negative potentials. This resulted in inward K^+ currents (Fig. 2) and then inactivating outward currents at more depolarized potentials (Fig. 3). In other experiments cells were held at a hyperpolarized potential where I_{KI} was not active and given a series of large depolarizing pulses of the same magnitude. Using a repetition rate of 1 pulse sec^{-1}, the first step in a series consistently resulted in a minimal current associated with a large inward tail current (Fig. 5*A*). Subsequent steps to the same voltage produced outward currents that rapidly reached a peak value followed by a slower decline (Fig. 5*A*). This suggested that K^+ was entering the cells following return to the holding potential (while the channels were still open and the driving force for K^+ was greatest), as evidenced by the large tail currents. Presumably K^+ accumulated inside the cell at the negative holding potential then left the cell during the depolarizing voltage step. This hypothesis was further tested by increasing the frequency of voltage steps. When the stimulus frequency was increased to 10 pulses sec^{-1}, currents increased gradually to a maximum value during repeated steps (Fig. 5*B*). This suggested that during initial steps there was less intracellular accumulation of K^+ between pulses and therefore less outward current during depolarizing steps. The outward current increased in size with repeated voltage steps until equilibrium was reached (Fig. 5*C*). Following several seconds at a holding potential of −97 mV, the instantaneous zero-current potential mea-

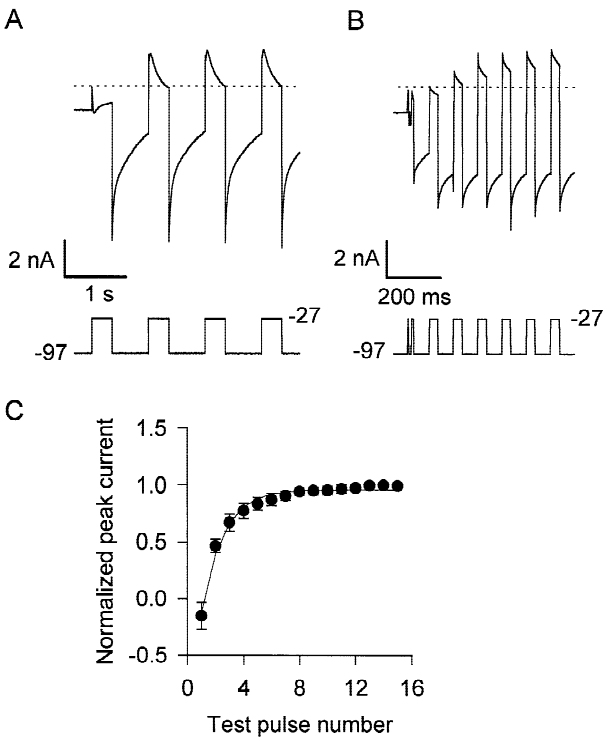

Fig. 5. Intracellular accumulation and depletion of K^+ during repeated pulses in Na^+-loaded cells. (*A*) Cell was held at −97 mV and given a 70 mV depolarizing voltage step four times. During the first step only a small inward current was apparent but a large tail current was present on stepping back to the holding potential. Subsequent steps evoked rapidly activating and inactivating currents. The initial depolarizing pulse presumably opened delayed rectifier channels allowing influx and intracellular accumulation of K^+ ions. The declining current during the next step could be attributed to egress and depletion of K^+ from the cell's interior. K^+ appeared to accumulate inside the cell between voltage steps. Holding current eventually returned to its initial value as shown in *B*. (*B*) The frequency of voltage steps was increased 10-fold and the step duration decreased. Outward currents and tail currents increased gradually with repeated voltage steps. A stimulus artifact was present at the onset of the pulse train. (*C*) The increase in peak outward current in response to repeated voltage steps is shown for 3 cells. The voltage protocol used is shown in *B*. Current values (mean ± SD) were normalized to the maximum value obtained for each cell during the protocol. The solid line represents a fit to the equation for a single exponential. In the experiments shown the electrode solution was $(Na^+)_{in}$ and $[K^+]_{out}$ was 5 mM.

sured in current clamp in this cell was −29 mV. After several seconds at a holding potential of +12 mV, the zero-current potential was +6 mV. This shift in zero-current was reversible and presumably occurred as a result of the changing K^+ distribution (*data not shown*). In summary, the simplest explanation for the results shown in Fig. 5 is that K^+ enters the cell through delayed rectifier channels, accumulates sufficiently to produce a substantial change in E_K and then carries outward current during subsequent depolarizations. The "inactivation" of the outward current could then be due to depletion of intracellular K^+.

K^+ Currents are Carried Through Delayed Rectifier Channels in the Presence of Intracellular Na^+

The source of K^+ for both the inward and outward currents therefore appeared to be the external solution. The negative activation range and characteristic kinetics suggested that the current was carried through I_{KI} channels. To further test this, the effect of 4-aminopyridine (4-AP), a known blocker of delayed rectifier currents in type I hair cells (Rennie & Correia, 1994; Rüsch & Eatock, 1996*a*), was investigated. Figure 6*A* demonstrates the effect of 4-AP on currents evoked when K^+ was present externally, but not included in the patch electrode solution. Control current (left), current during exposure to 2 mM 4-AP (center) and recovery (right) are shown. The *I-V* plot in Fig. 6*B* shows the effect of 4-AP over a range of potentials in the same cell. Both inward and outward currents are greatly reduced in the presence of 4-AP. Similar results were obtained in a total of 3 cells patch-clamped with $(Na^+)_{in}$ and exposed to 4-AP, with >80% block of the peak current seen at potentials between −10 and 0 mV. These results confirmed that inward currents were through delayed rectifier channels and were not due to calcium or inward rectifier currents.

External K^+ therefore plays a major role in the generation of the large currents seen in cells patch clamped with solutions containing Na^+. Owing to the presence of delayed rectifier conductance, the specific membrane conductance of type I cells can be as large as 50 nS/pF (Rüsch et al., 1998). Even in the absence of K^+ in the patch electrode solution it appears that significant intracellular loading of cells with K^+ can occur. At potentials between −90 and −50 mV this loading occurs as a result of K^+ entry through I_{KI} channels.

Cs^+ Permeability

Na^+ did not permeate through I_{KI} channels under any of the conditions tested, but type I cells showed significant permeability to Cs^+ in the absence of K^+ (Fig. 7*A*). The instantaneous component and deactivation of the current below −100 mV recorded under symmetrical Cs^+ conditions are typical of I_{KI} (Fig. 7*A*). When Cs^+-loaded cells were exposed to external solutions containing mixtures of Cs^+ and K^+, a reduction in inward current was observed. Figure 7*B* shows inward currents from a cell in 0 and 20 mM $[K^+]_{out}$ in the presence of internal and external Cs^+. The *I-V* relation for the steady-state currents from the same cell is shown in Fig. 7*C*. The inward current activates at potentials above −100 mV and currents in 20 mM K^+ (open symbols) are consistently smaller than currents recorded in the absence of external K^+ (filled symbols). The slope conductance, relative to the conductance in the absence of K^+, is plotted for dif-

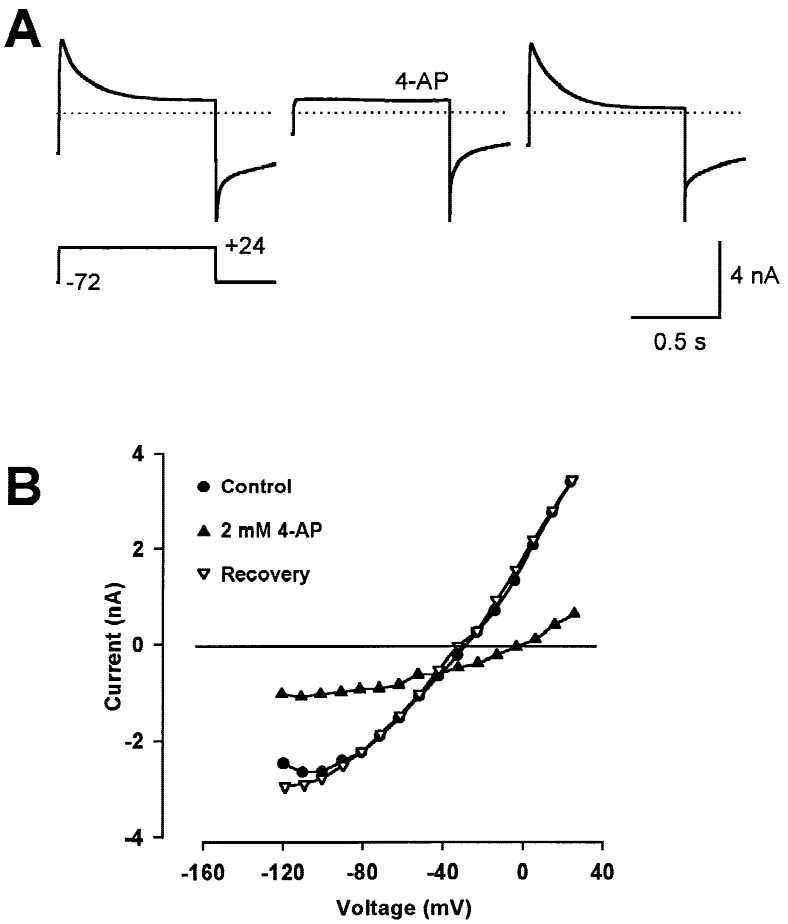

Fig. 6. Sensitivity of the K^+ current to 4-AP in Na^+-loaded cells. (*A*) Control current (left panel), current in the presence of 2 mM 4-aminopyridine (4-AP, center panel) and current during recovery (right panel) in response to a voltage step are shown. (*B*) Current-voltage relation showing control (filled circles), current in the presence of 2 mM 4-AP (filled triangles) and recovery (open triangles). Peak currents were measured. 4-AP reduces both inward and outward current components. The identity of the conductance remaining in the presence of 4-AP is not known, but since it reversed close to 0 mV it may be a leak conductance.

ferent concentrations of external K^+ in Fig. 7*D*. As the external K^+ concentration was increased the conductance values first decreased and then increased to a maximum in an external solution containing 155 mM K^+ and 5 mM Cs^+ with $(Cs^+)_{in}$ (Fig. 7*D*). The results indicate an anomalous mole fraction effect (Hille, 1992).

Discussion

Na^+ Does Not Permeate I_{KI} Channels

We have investigated the behavior of I_{KI} under a variety of ionic conditions and shown that even when K^+ is absent from the patch electrode solution, large currents can be recorded from isolated type I hair cells when external K^+ is present. These currents appear to be carried by K^+ through delayed rectifier channels, since they are kinetically similar to currents observed under normal K^+ conditions, they do not occur in the absence of external K^+ and are blocked by 4-AP.

Some neuronal K channels become highly permeant to Na^+ in the absence of external and internal K^+ (Zhu & Ikeda, 1993; Callahan & Korn, 1994; Kiss et al., 1998). In certain delayed rectifiers a cationic current was reported when intracellular K^+ was lowered to concentrations below 30 mM (Korn & Ikeda, 1995; Block & Jones, 1997). In contrast, Shaker B channels entered a collapsed state following membrane depolarizations in the absence of internal and external K^+ (Gomez-Lagunas, 1997). None of these mechanisms adequately explain our results obtained from I_{KI} channels under a variety of different ionic conditions. I_{KI} channels did not show significant permeability to Na^+, since there was very little current in the absence of K^+ with $(Na^+)_{in}$.

The inward currents observed between −40 and −90 mV with $(Na^+)_{in}$ and $(Cs^+)_{in}$ are due to K^+ entry. The outward currents above −40 mV with $(Na^+)_{in}$ also appear to be carried by K^+ suggesting that intracellular K^+ levels may rise by several mM as a result of K^+ entry and accumulation. Indeed the instantaneous zero-current potential following a prolonged hyperpolarization was much more negative than that following a prolonged depolarization. If we consider a type I cell simply as a cylinder of length (l) of 25.4 μm and an average radius (r) of 2.9 μm (based on length, cuticular plate and cell body measurements of pigeon type I hair cells, Ricci et

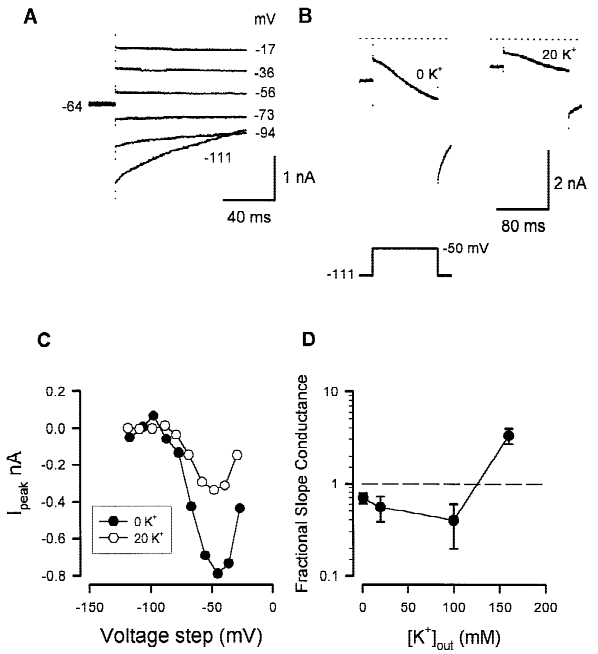

Fig. 7. Cs^+ blocks and permeates the delayed rectifier channel. (*A*) Currents recorded in near symmetrical Cs^+ (0 K^+) conditions. Cell was held at −64 mV and stepped through a range of potentials. The resting conductance and deactivation of the current at potentials negative to −100 mV are typical of I_{KI}. (*B*) Introduction of 20 mM K^+ to the external solution resulted in a reduction of the inward current. Responses to a voltage step in external solutions of 0 K^+/160 mM Cs^+ and 20 K^+/140 mM Cs^+ are shown. (*C*) The *I-V* relation shows peak currents in 0 K^+/160 mM Cs^+ (filled symbols) and 20 K^+/140 mM Cs^+ (open symbols). Records used for the *I-V* relation were leak-subtracted. (*D*) Mixtures of external Cs^+/K^+ result in a mole fraction effect. Each symbol represents the mean value from 3–6 cells with each cell providing data for at least 2 points at 1, 20, 100 and 155 mM external K^+. Total concentration of K^+ and Cs^+ in the external solution was 160 mM. Slope conductance was estimated from ramp protocols (*see* Materials and Methods) and normalized to the value in external 160 Cs^+/0 K^+ (dashed line). Electrode solution was $(Cs^+)_{in}$ for all cells.

al., 1997*b*), then the volume of the cell body ($\pi r^2 h$) is equivalent to 6.7×10^{-16} l. A reversal potential change of −29 to +6 mV (measured in the cell shown in Fig. 5) is predicted to change the intracellular K^+ molarity by 12 mM using the Nernst equation (assuming the membrane is permeable only to K^+). The change in the number of moles of K^+ ions inside the cell will then be 8.0×10^{-18}. By Faraday's constant (F, 9.648×10^4 C mol^{-1}) this gives a net charge of 7.7×10^{-13} *C*. Over a time period of 1 sec this would be equivalent to a steady current flow of 7.7×10^{-13} *A*, several orders of magnitude less than the currents reported here. Despite the low resistance of the patch electrode (≤2 MΩ) and the small size of these cells, which should result in a rapid dialysis of intracellular solution by the patch electrode solution, it therefore seems feasible that relatively high concentrations of K^+ could be achieved at a site adjacent to the channel.

A similar example of "K^+-loading" has been observed in Müller cells of the guinea pig retina (Francke et al., 1995). Like type I hair cells, Müller cells have a very low input resistance (10–20 MΩ) owing to a resting K^+ conductance and when patch electrode K^+ was replaced by NMDG and/or Cs^+, outward K^+ currents were still observed in the presence of 5 mM external K^+. However K^+ entry in Müller cells was through a K^+-selective inward rectifier. K^+ entry into type I hair cells appeared to be through I_{KI}, since the current activated above −90 mV and was blocked by 4-AP.

Cs^+ Permeates and Blocks I_{KI} Channels

Most K^+ channels are impermeant to Cs^+ but exceptions include the *A* current in guinea pig laterodorsal tegmental neurons (Sanchez, Surkis, & Leonard, 1998), a delayed rectifier in chick dorsal root ganglion neurons (Trequattrini, Petris & Franciolini, 1996) and I_{KI} in mammalian and avian type I vestibular hair cells (Griguer, Sans & Lehouelleur, 1993; Rennie & Correia, 1994; Rüsch & Eatock, 1996*a*). The permeability ratio, P_{Cs}/P_K, in all three cell types was approximately 0.3. The cloned delayed rectifier channel Kv2.1 became Cs^+-preferring following substitution of His for Ile at position 369. The mutated channel showed a greatly reduced sensitivity to block by external TEA as compared to the wild type (De Biasi, et al., 1993). I_{KI} is also relatively insensitive to external TEA (Rennie & Correia, 1994; Rüsch et al., 1996*a*). Externally applied Cs^+ has previously been shown to block inward currents through I_{KI} (Rennie & Correia, 1994; Rüsch & Eatock, 1996*a*) and we report here an anomalous mole fraction effect in mixtures of external K^+ and Cs^+. The competitive interaction between these two ions within the channel results in a minimum conductance and indicates a multi-ion pore. Anomalous mole fraction effects have been reported for many K^+ currents including $K_{(Ca)}$, inward rectifier and delayed rectifier (Hagiwara et al., 1977; Eisenmann, Latorre & Miller, 1986; Block & Jones, 1996, 1997; Yool & Schwarz, 1996; Trequattrini et al., 1996), but were absent for M currents (Block & Jones, 1996). Recent evidence suggests that competition within the K^+ channel pore for binding sites is an important determinant of ionic selectivity (Korn & Ikeda, 1995).

Kinetics

Currents carried through delayed rectifier channels have complex activation kinetics. For example, outward delayed rectifier currents in bullfrog sympathetic neurons have been fit with Hodgkin-Huxley-type kinetics with an order of 2 or 3 producing the best fit, but better fits were obtained with other kinetic schemes and an allosteric model gave the best overall fit (Klemic, Durand & Jones,

1998). The activation kinetics of outward current through type I hair cell delayed rectifier channels have previously been fit with the sum of two exponentials (Rüsch & Eatock, 1996*a*; Rüsch et al., 1998) or Hodgkin-Huxley kinetics with an order of 1 (Ricci et al., 1996). The activation of inward currents carried through I_{KI} were fit reasonably well with a first order scheme, but kinetics became increasingly complex with increasing activation of the current. Kinetic behavior of the inward currents was similar with K^+, Na^+ or Cs^+ in the patch electrode solution, suggesting that under these different conditions currents were consistently through I_{KI}.

Inactivation of outward currents with $(Na^+)_{in}$ followed a monoexponential time course as reported previously for $(Cs^+)_{in}$ and $(K^+)_{in}$ (Rüsch & Eatock, 1996*a*), but whereas complete inactivation was often seen with $(Na^+)_{in}$, only ~40% inactivation of the current was seen with $(K^+)_{in}$ under similar conditions. The relatively rapid inactivation under $(Na^+)_{in}$ conditions appears to be due to depletion of internal K^+.

Conclusion

A consistent pattern has emerged across species and vestibular end organs in which type I hair cells express a low voltage-activated K^+ channel present at high current density (Correia & Lang, 1990; Griguer et al., 1993; Rennie & Correia, 1994; Rüsch & Eatock, 1996*a*; Goldberg, 1996*a*; Ricci et al., 1996; Oghalai et al., 1998). I_{KI} has an unusually negative activation range and may equip type I hair cells with a low sensitivity, but fast frequency response (Rennie et al., 1996; Rüsch & Eatock, 1996*b*). It is likely that the basolateral membrane of type I hair cells is exposed to dramatic concentration changes of ions, notably K^+, during stimulation (Goldberg, 1996*a*,*b*). An increase in external K^+ during depolarization of a type I hair cell could therefore lead to a decrease in membrane resistance and a smaller membrane response to further stimuli. A vast diversity within the family of voltage-aged K^+ channels has become apparent over the last decade and in many systems the molecular structure and biophysical characteristics of a particular K^+ channel can now be reconciled with its physiological function (reviewed in Robertson, 1997). The molecular identity of I_{KI} remains to be ascertained, but knowledge of its permeation properties, such as its anomalous mole fraction behavior with Cs^+, should aid in its determination.

Thanks to Anthony Ricci, Ph.D. for helpful suggestions, Sara Black and Adrian Perachio, Ph.D. for access to their gerbil colony and Rosanne Heflin-Gorny for assistance with manuscript preparation. This research was supported by NIDCD grants DC03527 and DC03287 to KJR and in part by DC01273 to MJC.

References

Behrend, O., Schwark, T., Kunihiro, T., Strupp, M. 1997. Cyclic GMP inhibits and shifts the activation curve of the delayed rectifier (IK1) of type I mammalian vestibular hair cells. *Neuroreport* **8:**2687–2690

Block, B.M., Jones, S.W. 1996. Ion permeation and block of M-type and delayed rectifier potassium channels. *J. Gen. Physiol.* **107:**473–488

Block, B.M., Jones, S.W. 1997. Delayed rectifier current of bullfrog sympathetic neurons: ion-ion competition, asymmetrical block and effects of ions on gating. *J. Physiol.* **499:**403–416

Callahan, M.J., Korn, S.J. 1994. Permeation of Na^+ through a delayed rectifier K^+ channel in chick dorsal root ganglion neurons. *J. Gen. Physiol.* **104:**747–771

Correia, M.J., Lang, D.G. 1990. An electrophysiological comparison of solitary type I and type II vestibular hair cells. *Neurosci. Lett.* **116:**106–111

Correia, M.J., Ricci, A.J., Rennie, K.J. 1996. Filtering properties of vestibular hair cells: an update. *In*: New Frontiers of Vestibular Research. B. Cohen and S. Highstein, editors. *Ann. N.Y. Acad. Sci.* **781:**138–149

De Biasi, M., Drewe, J.A., Kirsch, G.E., Brown, A.M. 1993. Histidine substitution identifies a surface position and confers Cs^+ selectivity on K^+ pore. *Biophys. J.* **65:**1235–1242

Eisenman, G., Latorre, R., Miller, C. 1986. Multi-ion conductance in the high-conductance Ca^{2+}-activated K^+ channel from skeletal muscle. *Biophys. J.* **50:**1025–1034

Francke, M., Pannicke, T., Reichelt, W. 1995. Repetitive depletion and recovery of intracellular K^+ in retinal Muller glial cells during whole-cell voltage-clamp. *J. Neurosci. Meth.* **61:**169–184

Goldberg, J.M. 1996*a*. Transmission between the type I hair cell and its calyx ending. *In*: New Frontiers of Vestibular Research. B. Cohen and S. Highstein, editors. *Ann. N.Y. Acad. Sci.* **781:**474–488

Goldberg, J.M. 1996*b*. Theoretical analysis of intercellular communication between the vestibular type I hair cell and its calyx ending. *J. Neurophysiol.* **76:**1942–1957

Gomez-Lagunas, F. 1997. Shaker B K^+ conductance in Na^+ solutions lacking K^+ ions: a remarkably stable non-conducting state produced by membrane depolarizations. *J. Physiol.* **499:**3–15

Griguer, C., Sans, A., Lehouelleur, J. 1993. Non-typical K^+-current in cesium-loaded guinea pig type I vestibular hair cell. *Pfluegers Arch.* **422:**407–409

Hagiwara, S., Miyazaki, S., Krasne, S., Ciani, S. 1977. Anomalous permeabilities of the egg cell membrane of a starfish in K^+-$T1^+$ mixtures. *J. Gen. Physiol.* **70:**269–281

Hille, B. 1992. Ionic Channels of Excitable Membranes. Sinauer Associates, Sunderland, MA

Kiss, L., Immke, D., LoTurco, J., Korn, S.J. 1998. The interaction of Na^+ and K^+ in voltage-gated potassium channels. Evidence for cation binding sites of different affinity. *J. Gen. Physiol.* **111:**195–206

Klemic, K.G., Durand, D.M., Jones, S.W. 1998. Activation kinetics of the delayed rectifier potassium current of bullfrog sympathetic neurons. *J. Neurophysiol.* **79:**2345–2357

Korn, S.J., Ikeda, S.R. 1995. Permeation selectivity by competition in a delayed rectifier potassium channel. *Science* **269:**410–412

Oghalai, J.S., Holt, J.R., Nakagawa, T., Jung, T.M., Coker, N.J., Jenkins, H.A., Eatock, R.A., Brownell, W.E. 1998. Ionic currents and electromotility in inner ear hair cells from humans. *J. Neurophysiol.* **79:**2235–2239

Rennie, K.J., Correia, M.J. 1994. Potassium currents in mammalian and avian isolated type I semicircular canal hair cells. *J. Neurophysiol.* **71:**317–329

Rennie, K.J., Ricci, A.J., Correia, M.J. 1996. Electrical filtering in gerbil isolated type I semicircular canal hair cells. *J. Neurophysiol.* **75:**2117–2123

Ricci, A.J., Rennie, K.J., Correia, M.J. 1996. The delayed rectifier, I_{KI}, is the major conductance in type I vestibular hair cells across vestibular end organs. *Pfluegers Arch.* **432:**34–42

Ricci, A.J., Rennie, K.J., Cochran, S.L., Kevetter, G.A., Correia, M.J. 1997*a*. Vestibular type I and type II hair cells. 1: Morphometric identification in the pigeon and gerbil. *J. Vestibular Res.* **7:**393–406.

Ricci, A.J., Cochran, S.L., Rennie, K.J., Correia, M.J. 1997*b*. Vestibular type I and type II hair cells. 2: Morphometric comparisons of dissociated pigeon hair cells. *J. Vestibular Res.* **7:**407–420

Robertson, B. 1997. The real life of voltage-gated K^+ channels: more than model behavior. *Trends Pharmacol. Sci.* **18:**474–483

Rüsch, A., Eatock, R.A. 1996*a*. A delayed rectifier conductance in type I hair cells of the mouse utricle. *J. Neurophysiol.* **76:**995–1004

Rüsch, A., Eatock, R.A. 1996*b*. Voltage responses of mouse utricular hair cells to injected current. *In*: New Frontiers of Vestibular Research. B. Cohen and S. Highstein, editors. *Ann. N.Y. Acad. Sci.* **781:**71–84

Rüsch, A., Lysakowski, A., Eatock, R.A. 1998. Postnatal development of type I and type II hair cells in the mouse utricle: acquisition of voltage-gated conductances and differentiated morphology. *J. Neurosci.* **18:**7487–7501

Sanchez, R.M., Surkis, A., Leonard, C.S. 1998. Voltage-clamp analysis and computer simulation of a novel cesium-resistant A-current in guinea pig laterodorsal tegmental neurons. *J. Neurophysiol.* **79:** 3111–3126

Trequattrini, C., Petris, A., Franciolini, F. 1996. Characterization of a neuronal delayed rectifier K current permeant to Cs and blocked by verapamil. *J. Membrane Biol.* **154:**143–153

Wersäll, J. 1956. Studies on the structure and innervation of the sensory epithelium of the cristae ampullares in the guinea pig. *Acta Otolaryngol. Suppl.* **126:**1–85

Yool, A.J., Schwarz, T.L. 1996. Anomalous mole fraction effect induced by mutation of the H5 pore region in the Shaker K^+ channel. *Biophys. J.* **71:**2467–2472

Zhu, Y., Ikeda, S.R. 1993. Anomalous permeation of Na^+ through a putative K^+ channel in rat superior cervical ganglion neurones. *J. Physiol.* **468:**441–461